ELSEVIER
Journal of Contaminant Hydrology 53 (2001) 199–232
JOURNAL OF
Contaminant
Hydrology
www.elsevier.com/locate/jconhyd

Assessing the natural attenuation of organic contaminants in aquifers using plume-scale electron and carbon balances: model development with analysis of uncertainty and parameter sensitivity

Steven F. Thornton *, David N. Lerner [1], Steven A. Banwart [2]

Groundwater Protection and Restoration Group, Department of Civil and Structural Engineering, University of Sheffield, Mappin St., Sheffield S1 3JD, UK

Received 9 February 2000; received in revised form 13 October 2000; accepted 7 February 2001

Abstract

A quantitative methodology is described for the field-scale performance assessment of natural attenuation using plume-scale electron and carbon balances. This provides a practical framework for the calculation of global mass balances for contaminant plumes, using mass inputs from the plume source, background groundwater and plume residuals in a simplified box model. Biodegradation processes and reactions included in the analysis are identified from electron acceptors, electron donors and degradation products present in these inputs. Parameter values used in the model are obtained from data acquired during typical site investigation and groundwater monitoring studies for natural attenuation schemes. The approach is evaluated for a UK Permo-Triassic Sandstone aquifer contaminated with a plume of phenolic compounds. Uncertainty in the model predictions and sensitivity to parameter values was assessed by probabilistic modelling using Monte Carlo methods. Sensitivity analyses were compared for different input parameter probability distributions and a base case using fixed parameter values, using an identical conceptual model and data set. Results show that consumption of oxidants by biodegradation is approximately balanced by the production of CH_4 and total dissolved inorganic carbon (TDIC) which is conserved in the plume. Under this condition, either the plume electron or carbon balance can be used to determine contaminant mass loss, which is equivalent to only 4% of the estimated source term. This corresponds to a first order, plume-averaged, half-life of >800 years. The electron balance is particularly sensitive to uncertainty in the

---

* Corresponding author. Fax: +44-114-222-5700.

E-mail addresses: S.F.Thornton@sheffield.ac.uk (S.F. Thornton), D.N.Lerner@sheffield.ac.uk (D.N. Lerner), S.A.Banwart@sheffield.ac.uk (S.A. Banwart).

[1] Fax: +44-114-222-5701.

[2] Fax: +44-114-222-5700.

PII: S0169-7722(01)00167-X

source term and dispersive inputs. Reliable historical information on contaminant spillages and detailed site investigation are necessary to accurately characterise the source term. The dispersive influx is sensitive to variability in the plume mixing zone width. Consumption of aqueous oxidants greatly exceeds that of mineral oxidants in the plume, but electron acceptor supply is insufficient to meet the electron donor demand and the plume will grow. The aquifer potential for degradation of these contaminants is limited by high contaminant concentrations and the supply of bioavailable electron acceptors. Natural attenuation will increase only after increased transport and dilution.

Keywords: Natural attenuation; Biodegradation; Phenol; Groundwater; Risk assessment; Monte Carlo

1. Introduction

There is an increasing acceptance of risk-based approaches to groundwater protection and restoration, provided that there is no demonstrable harm to potential receptors. Natural attenuation (NA) processes can effectively remediate contaminated groundwater (Nicholson et al., 1983; Lyngkilde and Christensen 1992; Christensen et al., 1994). Natural attenuation is the effect of naturally occurring physical, chemical and biological processes that reduce the load, concentration, flux or toxicity of polluting substances in groundwater (Environment Agency, 2000). Performance evaluation of NA commonly includes deterministic analysis, using numerical or analytical groundwater flow and solute transport models to predict future plume behaviour and to assess the risk of plume migration at a downgradient receptor (Ravi et al., 1997). A problem encountered in all predictive modelling is uncertainty in the parameter values used as inputs in the model simulations. In solute transport studies, this uncertainty arises from a variety of sources, recently reviewed in Abbaspour et al. (1998). These include the heterogeneity in subsurface depositional and geochemical environments, which produces spatially variable hydrogeological, geological and hydrochemical characteristics. This results in a range in possible transport parameters (groundwater velocity, aquifer hydraulic conductivity and gradient, porosity, dispersivity) (Gelhar et al., 1992) and solute concentrations, which define contaminant distributions. It is usually possible to undertake only limited sampling of the value and range in these site-specific properties in most site investigation and groundwater monitoring studies, resulting in incomplete information regarding their spatial and temporal variability (James and Oldenburg, 1997; McNab and Dooher, 1998). Additional uncertainty arises from incomplete understanding of the plume source term characteristics, including contaminant source location(s), release history and spill mass (McNab and Dooher, 1998; Skaggs and Kabala, 1998).

The uncertainty in parameter inputs for solute transport models creates cumulative uncertainties in the anticipated plume behaviour. Because models are calibrated to existing or historical pollutant concentration data, uncertainty in the system parameters results in a non-unique prediction of contaminant fate (McNab and Dooher, 1998). These uncertainties may be large, variable, and as important in the risk assessment process as the contaminant concentration estimates (James and Oldenburg, 1997). Extensive data collection (site, investigation, monitoring and sampling) is normally required to reduce parameter uncertainty (McNab and Dooher, 1998). However, short-term studies cannot usually wait to evaluate trends from field data and need to predict contaminant fate in a general context. If estimates of biodegradation and possible limiting factors can be obtained from basic field studies, then simple predictions of environmental risk may be possible. Protocols have been developed to evaluate the performance of monitored NA schemes (e.g. Buscheck and O'Reilly, 1995; Wiedemeier et al., 1995) but these may be difficult to apply at sites with complex source histories and results may be influenced by the design of monitoring borehole networks (Schreiber and Bahr, 1999). This guidance also only provides an indirect estimate of contaminant mass loss using rate constants obtained from limited groundwater monitoring. Rate constants derived on this basis may therefore neglect the variability in solute concentration and their reliability cannot be determined (Ravi et al., 1997). Significant improvements in process understanding and assessment of contaminant fate can be achieved from mass balance studies of pollutant transformation at laboratory-scale, where variability in the system parameters can be controlled and closely monitored (Hess et al., 1996; Hunkeler et al., 1998). This has seldom been attempted in field studies of pollutant fate (e.g. Hunkeler et al., 1999) where heterogeneity and uncertainty need to be taken into account to perform a representative risk assessment (Goodrich and McCord, 1995; McNab and Dooher, 1998).

This paper presents a quantitative methodology for the field-scale performance assessment of NA using plume-scale electron and carbon balances. The methodology developed provides a practical framework for the calculation of global mass balances for contaminant plumes, using a suite of governing equations and biodegradation processes as inputs in a simplified box model. Processes included in the analysis and parameter values used in the model inputs are obtained from basic data that is acquired during a typical site investigation and groundwater monitoring study for NA schemes. The focus of the study is to evaluate the box model as an improved site investigation tool for the risk-based restoration of contaminated aquifers using NA. The approach is evaluated for a site on a UK sandstone aquifer contaminated with a large plume of phenolic compounds. The advantages of the model over existing approaches for calculating plume mass balances are that mass balances are estimated using all monitoring wells over the scale and history of the plume, uncertainty in model inputs is formally evaluated and included in model predictions, and sources of uncertainty in model predictions are identified, to target further site investigation. The specific objectives of the study are:

(a) to assess the feasibility of taking a holistic view of contaminant plumes to evaluate the potential for NA at fieldscale;
(b) to examine the value of electron and carbon balances in providing an estimate of the magnitude of biodegradation processes, contaminant turnover, plume status and constraints on system performance for the site under study;
(c) to understand the effects of variability in parameter inputs on the robustness of the model and identify the key parameters responsible for uncertainty in the performance prediction for NA at the site.

The third objective is examined using Monte Carlo analysis to generate forecast predictions for the input parameters in the model. Sources of uncertainty in model forecasts are identified from parameter sensitivity analyses.

2. Monte Carlo analysis and modelling approach

Parameter uncertainty in environmental studies is conveniently assessed by stochastic simulation using Monte Carlo methods. User-specified probability distributions are defined for model parameters, to create a known or assumed range in the parameter value and to represent the uncertainty in that parameter. Uncertainty in all the parameter inputs is propagated through the model to produce a stochastic simulation, in which many forecast predictions are produced, rather than a single output based on a set of average input values. Monte Carlo analysis is commonly employed in environmental risk assessments (Jefferies et al., 1993). The technique has been used to examine the fate of pollutants released from waste disposal sites (Eschenroeder and Faeder, 1988; Goodrich and McCord, 1995; Hass et al., 1996; Abbaspour et al., 1998), petroleum hydrocarbon and chlorinated solvent spillages (James and Oldenburg, 1997; McNab and Dooher, 1998), and to evaluate controls on contaminant plume source terms (Skaggs and Kabala, 1998).

Sensitivity analyses provide insight into the impact of parameter probability distributions on the uncertainty in forecast variability. Parameters (independent variable) and forecasts (dependent variable) are rank-correlated by linear regression to quantify sensitivity. Correlation coefficients are tallied for each forecast and normalized to provide a relative contribution of each parameter to the variance in the corresponding forecast (McNab and Dooher, 1998).

In this study, Monte Carlo analyses were performed using a commercial software package, Crystal Ball® (Decisioneering, 1996). The effect of uncertainty in model input parameters was evaluated by comparing Monte Carlo forecasts predicted in three different scenarios against the results of a base case, developed using fixed input parameter values. The same conceptual model and site data were used in all scenarios, but the probability distributions assigned to parameter inputs were changed in the Monte Carlo simulations. The Monte Carlo simulations were run for 10,000 iterations and the significance of the forecasts was evaluated at the 95% confidence interval. This range approximately represents two standard deviations about the mean and is the conventional point examined in risk analyses in order to be conservative (James and Oldenburg, 1997; Ravi et al., 1997).

3. Case study

3.1. Site characteristics and investigation history

The site is an organic chemicals manufacturing plant constructed in 1950, which produces a range of organic chemicals, originally from coal-tar, but more recently from feedstocks. It is located 10 km north of Wolverhampton in the English West Midlands and overlies the Permo-Triassic Sherwood Sandstone, the second most important aquifer in the UK (Fig. 1). Locally, the aquifer is a fluviatile red-bed sandstone with a porosity of about 26% and bulk hydraulic conductivity of about 0.7 m day^{-1} (Aspinwall and Co., 1992). The aquifer sediments contain Fe and Mn oxides as grain coatings and minor particulate organic carbon. Background groundwater is aerobic. The water table is less than 5 m

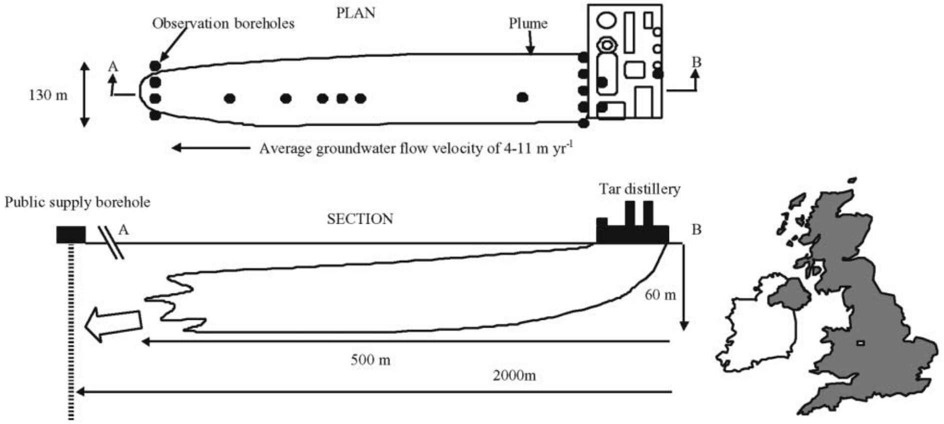

Fig. 1. Schematic plan and section of the site, showing location in UK, general observation wells and approximate location of plume (10 mg l^{-1} phenol).

below ground level (mbgl) and the aquifer is 250 m thick in the vicinity of the site. Groundwater flow is westerly at 4–11 m $year^{-1}$. The only receptor at risk is a public supply borehole, located approximately 2 km west of the plant and >100 years travel time from the present plume.

A plume of phenolic compounds (phenol, cresols and xylenols) which is the focus of this study was discovered under the site in 1987. The initial site investigation used 22 boreholes, typically nested in groups of three, terminating at different depths and many completed with 10-m screens. The plume developed using data from these boreholes extends approximately 500 m westward and to a depth of 50 m, when defined by the 10 mg l^{-1} phenol contour (Fig. 1). The total concentration of organic compounds in the source area is presently 24,800 mg l^{-1}, including 12,500 mg l^{-1} phenol. Site history and groundwater flow patterns suggest that spillages started soon after construction of the plant, that is, the plume is 47 years old. These spillages include mixtures of organic compounds, Cl from de-icing activities, NaOH from alkali storage facilities and SO_4 from mineral acid spills. These species form separate and overlapping plumes with the phenolics (Williams et al., in press). There is no information to indicate when spillages stopped, although the organic plume remains anchored by a strong source. This plume is bounded to the north by another plume, and the distinction between the two is based on contrasting contaminant compositions with different known source areas (Aspinwall and Co., 1992).

3.2. Data availability

The data used in the plume box model includes the aquifer physical properties (porosity, dispersivity), hydrogeological characterisitics (hydraulic conductivity, hydraulic gradients) and groundwater quality data (contaminant and inorganic solute distributions) obtained from the consultants' site investigation and groundwater modelling studies

(Aspinwall and Co., 1992). The history of spillages at the site cannot be accurately determined from the site records. There is no detailed information regarding the composition, timing, location and spatial extent of chemical spillages. Estimates of the possible range of spill areas have therefore been made from current site practices.

3.3. Groundwater sampling and chemical analysis

Two groundwater quality surveys were undertaken during the present study to provide additional hydrochemical data for the box model evaluation. Groundwater samples were collected in a closed system using dedicated bladder pumps after stabilisation of chemical parameters. Field measurements of pH, electrical conductivity (E.C.), redox potential (Eh), dissolved oxygen (D.O.) and temperature (°C) were made in a flow cell using electrodes. Interference from the high concentrations of organic pollutants resulted in false positive values of D.O. in the plume profile. Measurements of D.O. in the plume are expected to be below detection limits in the presence of measurable dissolved sulphide and Fe. Alkalinity was measured in $10 \times$ diluted unfiltered samples by colorimetric titration using standardised 1.6 N H_2SO_4 to a pH 4.5 end point (Hach Chemical Co.). Modelling of the groundwater hydrochemistry indicated that the phenolic compounds are present in undissociated form under the pH conditions in the plume (Thornton et al., submitted for publication) and that the measured alkalinity is derived from inorganic species (Mayer et al., 2001). Filtered samples (Whatman® 0.45 μm nylon) were obtained under N_2-pressure for analysis of Ca, Mg, K, Na, NH_4, Al, Si, Mn^{2+}, Fe^{2+}, Cl, NO^{2-}, NO^{3-}, PO_4^{3-} SO_4, S^{2-}, total organic carbon (TOC) and phenolic compounds. Samples for analysis of metals were preserved with 15% v/v nitric acid. Samples for the analysis of dissolved sulphides were preserved with NaOH. TOC was measured by combustion to CO_2 after removal of inorganic carbon by acidification. Cations (Ca, Mg, K, Na, Fe, Mn, Al), Si and S^{2-} were determined by inductively coupled plasma spectrophotometry, using a Spectro Flame M120 instrument, with a detection limit of 0.01 mg l^{-1} and precision of $\pm 2\%$. Anions (Cl, NO_2, NO_3, SO_4, PO_4) and NH_4 were determined by ion chromatography using a Dionex 2000 system with a detection limit of 1 mg l^{-1} and precision of $\pm 3\%$. Analyses for phenol, *o*-cresol, *m*/*p*-cresol, 2,3-xylenol, 2,4/2,5-xylenol, 2,6-xylenol, 3,5-xylenol and 3,6-xylenol were performed by high-pressure liquid chromatography, using a Gilson HPLC instrument. The detection limit and precision for the analysis of the phenolic compounds was 1 mg l^{-1} and $\pm 5\%$, respectively. Samples for dissolved gases (O_2, CO_2, CH_4, N_2) were collected in gas-tight steel bombs. Estimates of total dissolved inorganic carbon (TDIC) were obtained from dissolved CO_2 analyses using standard carbonate equilibria (Stumm and Morgan, 1996).

3.4. Groundwater chemistry and biodegradation processes

The distribution of phenol and other selected groundwater quality data collected from the existing monitoring boreholes is shown in Fig. 2. Contour plots were developed for all reactive species using the groundwater quality data for the monitoring boreholes (Table 1) and reactive transport modelling of the plume (Mayer et al., 2001). Background groundwater from upstream of the site (BH3d) is aerobic and contains NO_3 and SO_4, indicating

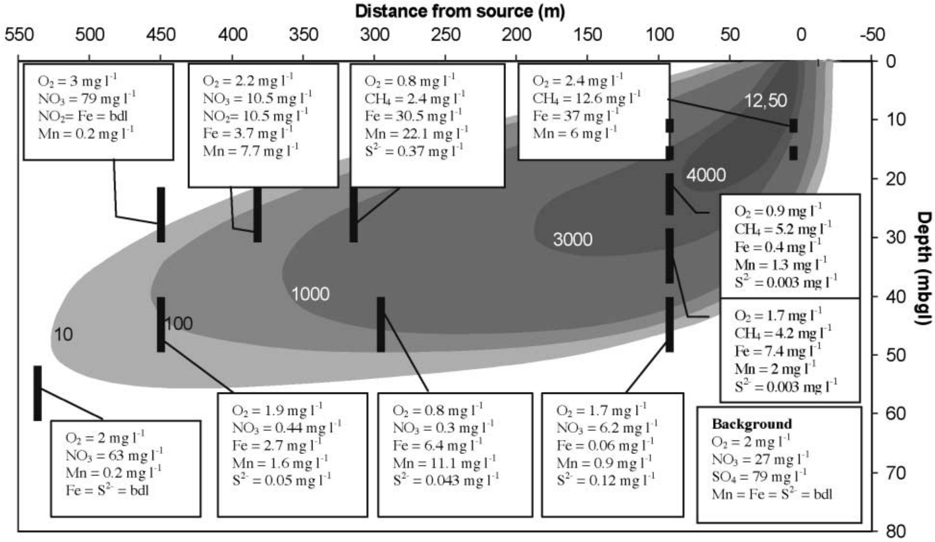

Fig. 2. Schematic cross-section of phenol plume with selected groundwater quality data (all concentrations in mg l^{-1}). Monitoring borehole locations and screen length are shown by black bars. Values of NO_3 below detection limits are omitted from monitoring boreholes.

that oxidant consumption due to natural organic matter or reduced solid phases is low in the uncontaminated aquifer. Organic contaminant concentrations (represented by phenol) decrease along the plume flow path and at the plume fringe, relative to the core. Contoured plots for dissolved Cl are not shown, but elevated Cl concentrations occur in the plume as a result of de-icing activities at the site (Table 1). The limit of Cl migration corresponds closely with that of the phenol plume, suggesting that there has been negligible retardation of the phenol by sorption to the aquifer solids. Consumption of aqueous and mineral oxidants in the plume is identified by corresponding increases in the concentrations of reduced inorganic species (NO_2^-, Mn^{2+}, Fe^{2+}, S^{2-}) and gases (CH_4), relative to the background groundwater. Concentrations of dissolved O_2 and N_2 in the plume are, respectively, below and above background groundwater levels (Table 1). The plume also contains elevated concentrations of TDIC, relative to background groundwater (Fig. 3). These data indicate that biodegradation of the organic contaminants is occurring under aerobic, NO_3-reducing, Mn-reducing, Fe-reducing, SO_4-reducing and methanogenic conditions, with the production of dissolved inorganic carbon and methane.

4. Development of plume box model

4.1. Governing reactions and assumptions

The mass and electron balance for the plume is calculated using redox half reactions. These are presented in Table 2 for reactions, which donate and accept electrons. The

Table 1
Groundwater chemistry for monitoring boreholes (Aug. 1997)

BH[a]	Distance[b]	Screen[c]	Pump[d]	Pump type[e]	pH	EC[f]	Eh[g]	T °C	D.O	Alkalinity[h]	Cl	NO_3	NO_2	NH_4	PO_4	SO_4	S^{2-} [i]	Fe^{2+}	Mn^{2+}
3d	Upstream	16.1–7.1	16.6	B	5.1	381	472	8	2	6.5	27	22	bdl	bdl	bdl	65	bdl	0.01	0.2
8m	0	10.4–11.4	10.9	I	5.8	1668	174	10	0.9	244	180	3.5	bdl	bdl	bdl	293	4	37	6
8d	0	16–17	16.5	I	5.8	1334	180	9	2.4	210	220	0.9	bdl	bdl	bdl	200	3	24	3
9m	100	10.4–11.4	10.9	I	9.5	4690	234	11	1.6	2090	130	bdl	bdl	bdl	54	237	10	4	0.2
9d	100	16–17	16.5	I	6.6	1209	243	11	0.9	345	37	0.9	bdl	bdl	7.5	91	bdl	0.4	1.3
13	100	41.5–53	47.3	B	7.3	725	310	11	1.7	210	44	6.2	bdl	bdl	bdl	66	122	0.1	0.9
14	100	30.5–42	36.2	B	5.9	794	277	10	0.6	115	54	2.6	bdl	bdl	bdl	155	7	3	7
15	100	24–33	28.5	B	5.5	500	225	7	1.7	95	17	0.3	2.3	bdl	bdl	60	bdl	7.4	2
40	315	21.6–30.4	26.5	B	5.5	1717	182	7	0.8	270	120	0.3	bdl	bdl	bdl	374	bdl	31	22
41	445	21.7–30.5	26.2	B	5.1	609	371	8	3	11	30	79	bdl	bdl	bdl	96	bdl	0.02	0.2
43	300	38.9–50.6	44.7	B	6.3	1480	−7	9	0.8	510	161	0.3	bdl	bdl	bdl	43	11	6.7	11
44	445	40.3–52	46.3	B	6.9	1240	131	9	1.9	482	76	0.4	bdl	bdl	bdl	46	211	2.7	1.6
55	385	21.2–30	25.6	B	5.5	783	76	9	2.2	86	41	11	11	bdl	bdl	178	7	3.7	8
57	535	50–60	55	B	5.3	725	412	8	2	80	49	63	bdl	bdl	bdl	87	bdl	0.01	0.2

	TOC	phenol	cresols	xylenols	TDIC	CO_2	CH_4	N_2	Ca	Mg	Na	K	Si	Al
3d	5	bdl	0.07	0.01	30	103	bdl	30	23	16	14	6.3	6.9	0.12
8m	14,910	12,509	8754	2349	93	314	0.4	63	79	55	314	4.8	4.4	1.4
8d	14,550	8587	8939	1682	79	265	12.6	38	55	19	266	4.3	6.7	2
9m	26	534	428	158	301	0.7	10.8	39	12	0.8	1769	3.3	0.9	0.4
9d	6214	3978	3519	2225	110	185	5.2	25	23	9.6	306	4.3	5.7	0.1
13	6.4	1	2	1.1	45	28	0.02	36	130	2.0	17	2.3	7.2	0.02
14	4463	2650	2205	542		232	1.5	88	99	16	42	3.8	7.2	0.04
15	5236	3869	2681	743	137	446	4.2	48	23	9.2	68	4.1	5.7	0.02
40	2008	1252	1249	243	481	1550	2.4	39	182	54	118	6.8	6.1	0.09
41	2	0.02	0.06	0.02	20	70	bdl	34	72	19	7.5	7.8	5.7	0.03
43	1183	1225	831	135	214	420	0.1	34	265	11	31	7.1	12	0.12
44	601	38	32	3	145	220	0.9	416	216	5.2	36	27	11	0.09
55	214	163	172	31	184	595	0.2	41	97	27	15.2	7.8	5.9	0.06
57	9.2	0.4	0.3	0.03	25	129	bdl	28	88	17	23	6.5	5.6	0.03

[a] BH3d is upstream of the site and “m” and “d” refer to “mid” and “deep” levels of a nested piezometer borehole.

[b] Distance in meters along plume flowpath of monitoring borehole from site source area borehole (BH8).

[c] Screen interval of monitoring borehole, in meters below ground level.

[d] Position of pump sampling inlet within monitoring borehole screen, in meters below ground level.

[e] Pumping mechanism used to recover groundwater samples (I, Inertial lift pump; B, Bladder pump).

[f] Electrical conductivity in $\mu S\ cm^{-1}$.

[g] Oxidation–reduction potential in mV relative to the standard hydrogen electrode.

[h] Alkalinity in $mg\ l^{-1}$ $CaCO_3$.

[i] Values in $\mu g\ l^{-1}$. All values in $mg\ l^{-1}$ unless stated otherwise.

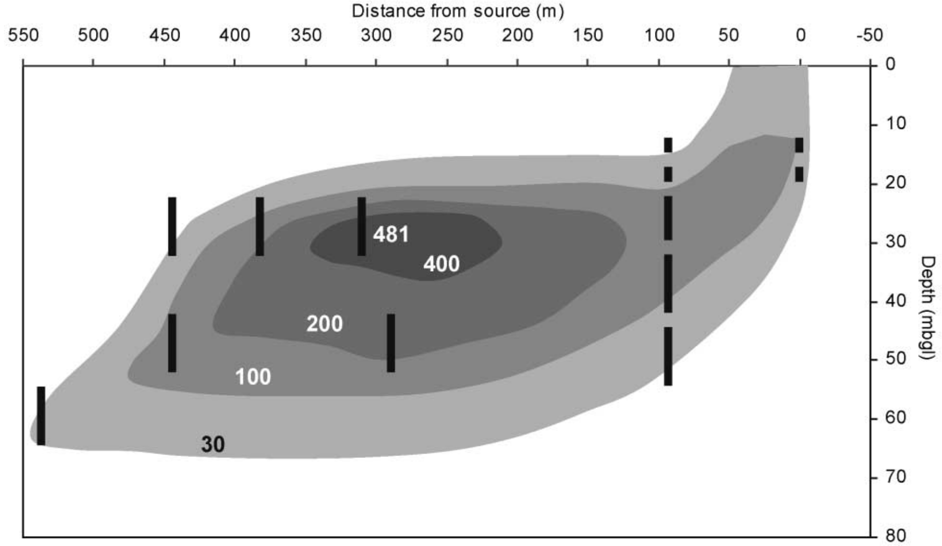

Fig. 3. Contours of total dissolved inorganic carbon concentration in the plume (mg l^{-1}), with monitoring borehole locations and screen length shown by black bars.

reactions include oxidation of organic electron donors (ED), represented by the main contaminants in the plume. The range of electron acceptors (EA) chosen includes the soluble and mineral oxidants, which participate in the oxidation of the organic fractions, based on hydrochemical data from the plume and uncontaminated groundwater. The half

Table 2
Redox half reactions used in the calculation of plume electron balance

Electron donating reactions
Oxidation of organic fractions

phenol: $C_6H_6O + 11H_2O \rightarrow 6CO_2 + 28e^- + 28H^+$
cresols: $C_7H_8O + 13H_2O \rightarrow 7CO_2 + 34e^- + 34H^+$
xylenols: $C_8H_{10}O + 15H_2O \rightarrow 8CO_2 + 40e^- + 40H^+$
TOC: $CH_2O + H_2O \rightarrow CO_2 + 4e^- + 4H^+$

Electron accepting reactions
Reduction of aqueous and mineral oxidants

dissolved oxygen: $O_2 + 4e^- + 4H^+ \rightarrow 2H_2O$
dissolved nitrate (nitrate reduction): $NO_3^- + 2e^- + 2H^+ \rightarrow NO_2^- + H_2O$
dissolved nitrate (denitrification): $NO_3^- + 5e^- + 6H^+ \rightarrow (1/2)N_2 + 3H_2O$
dissolved sulphate: $SO_4^{2-} + 8e^- + 8H^+ \rightarrow S^{2-} + 4H_2O$
dissolved carbon dioxide (methanogenesis): $CO_2 + 8e^- + 8H^+ \rightarrow CH_4 + 2H_2O$
solid phase manganese oxide: $MnO_2 + 2e^- + 4H^+ \rightarrow Mn^{2+} + 2H_2O$
solid phase iron oxide: $FeOOH + e^- + 3H^+ \rightarrow Fe^{2+} + 2H^2O$

reactions are written with CO_2 as the end product for oxidised organic carbon. This is an expected inorganic metabolite of degradation (Hess et al., 1996; Hunkeler et al., 1998) and is consistent with the elevated levels of dissolved CO_2 found in the plume during the groundwater quality surveys. The dissolved CO_2 will be speciated into other forms of inorganic carbon, although hydrochemical modelling (see Discussion) suggests that dissolved CO_2 is present primarily in H_2CO_3 and HCO_3^- forms in most boreholes sampled in the plume. All forms of CO_2 are included in the analysis for TDIC. Fermentation reactions in which organic compounds may function as both the ED and EA, and which involve no electron transfer, are not explicitly included in electron balance. However, the contribution of fermentation may be evaluated if the electron balance can be sufficiently constrained. Methane produced in the plume is assumed to have originated from biogenic reduction of dissolved CO_2, as opposed to fermentation of organic acid fractions (Chapelle, 1993). Therefore, the amount of CO_2 consumption attributable to methanogenesis by CO_2-reduction must be considered a maximum, and higher than that arising from direct methanogensis of the phenols (Table 3). The degradation of intermediate organic compounds, such as organic acids, is not considered in the case study evaluation, as no data were available for these compounds. However, these species can be included in the mass balance for the box model, as appropriate. It is also assumed that there are no inhibitions to degradation under each redox condition. No consideration is given to redox reactions other than those listed in Table 2, or to abiotic reactions, which may occur for some species (e.g. formation of FeS phases via direct reduction of Fe oxides by S^{2-}). The redox half reactions can be coupled to generate a complete reaction involving the oxidation of an ED species by an EA. A summary of the full reactions for ED and EA and for the oxidation processes identified in the plume is presented in Table 3 using phenol as the model compound.

4.2. Conceptual box model for plume

The reactions introduced above are incorporated with physical mass transport processes to produce a box model for the aquifer to calculate electron and mass balances for the contaminant plume. A schematic of this box model is shown in Fig. 4. The box model includes four input terms, which represent components from the background groundwater (BG), contaminant source term (ST), transverse dispersion (HT, VT) and plume residual fractions (PR). These terms are explained in Table 4. The background groundwater input

Table 3
Summary of degradation processes for phenol

Aerobic oxidation: $C_6H_6O + 7O_2 \rightarrow 6CO_2 + 3H_2O$
Reduction of nitrate: $C_6H_6O + 14NO_3^- \rightarrow 6CO_2 + 14NO_2^- + 3H_2O$
Denitrification: $C_6H_6O + (28/5)NO_3^- + (28/5)H^+ \rightarrow 6CO_2 + (14/5)N_2 + (29/5)H_2O$
Reduction of sulphate: $C_6H_6O + (7/2)SO_4^{2-} \rightarrow 6CO_2 + (7/2)S^{2-} + 3H_2O$
Reduction of solid phase Mn oxide: $C_6H_6O + 14MnO_2 + 28H^+ \rightarrow 6CO_2 + 14Mn^{2+} + 17H_2O$
Reduction of solid phase Fe oxide: $C_6H_6O + 28FeOOH + 56H^+ \rightarrow 6CO_2 + 28Fe^{2+} + 45H_2O$
Methanogenesis (fermentation): $C_6H_6O + 4H_2O \rightarrow (5/2)CO_2 + (7/2)CH_4$

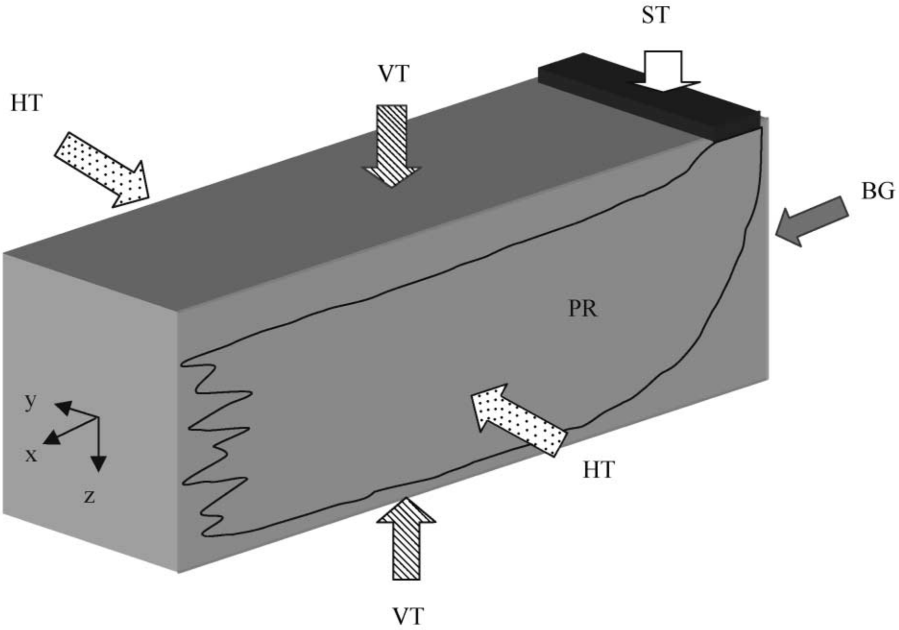

Fig. 4. Schematic of box model for calculation of plume electron balances (see Table 3 for explanation of symbols).

originates from advection into the rear of the plume, whereas the dispersive input arises from mixing of contaminated and uncontaminated background groundwater at the plume fringe. All components include an ED and EA input, where these are appropriate. The transverse dispersion input includes horizontal and vertical components (Fig. 4). However, the plume under study is bounded at the north margin by another plume, so that transverse dispersive inputs (e.g. of soluble EA) from this direction can be ignored. Hence, only horizontal dispersive inputs from the southern margin of the plume were included in the electron balance calculations. Calculation of the electron balance assumes that steady-state conditions exist for the source term and hydrogeological regime over the reference period of the plume (47 years).

4.3. Range and origin of input parameters

The range and origin of the parameter values used as inputs for the scenarios examined in the box model is presented in Table 5. These ranges include a minimum, likely and maximum value of each parameter. The minimum and maximum value of each parameter represents the range in the measured property or estimate, and the likely value is the mean of this range. Exceptions to this include the background groundwater concentration of dissolved oxygen where the likely value is a measured value falling within a theoretical range. The three inputs are identical in those cases where only one value of the measured parameter is available (e.g. background TDIC concentration, horizontal and vertical

Table 4
Nomenclature of input terms for plume box model

Input notation	Input term	Parameter	Comment
Source term (ST)	$I \times A_{\text{source}} \times C_{\text{source}} \times T$	I	Infiltration
		A_{source}	Area of contaminant spillage at source
		C_{source}	Concentration of spilled contaminant
		T	Reference time or age of plume
Background groundwater (BG)	$n_{\text{k}} \times \text{vel}_{\text{x}} \times A_{\text{rear}} \times C_{\text{oxidant}} \times T$	n_{k}	Aquifer kinematic porosity
		vel_{x}	Horizontal linear velocity
		A_{rear}	Rear cross sectional area of plume
		C_{oxidant}	Concentration of soluble oxidant
Horizontal transverse (HT)	$n_{\text{k}} \times \text{vel}_{\text{x}} \times \alpha_{\text{y}} \times A_{\text{transverse}} \times \delta C_{\text{oxidant}}/\delta y \times T$	$A_{\text{transverse}}$	Transverse sectional area of plume
		α_{y}	Horizontal transverse dispersivity
		$\delta C_{\text{oxidant}}/\delta y$	Oxidant concentration gradient at plume fringe
Vertical transverse (VT)	$2 \times n_{\text{k}} \times \text{vel}_{\text{x}} \times \alpha_{\text{z}} \times A_{\text{plan}} \times \delta C_{\text{oxidant}}/\delta y \times T$	A_{plan}	Plan cross-sectional area of plume
		α_{z}	Vertical transverse dispersivity
Plume residuals (PR)	$n_k \times \int C_{\text{residual}} \delta V$	C_{residual}	Concentration of residual species
		δV	Volume of aquifer between solute contours

Notes: Horizontal transverse input of oxidants occurs for south (one) side of plume only, whereas vertical transverse input occurs for upper and lower (two) sides of plume (see text).

Table 5
Summary of input parameters for plume box model

Parameter	Value			Comments
	Minimum	Likely	Maximum	
Plume dimensions				
Width (m)	131	131	131	Based on groundwater chemistry and configuration of source area
Length (m)	525	525	525	Present distance of migration
Depth (m)	40	40	40	Present depth below water table
Plume source strengths				
$\text{Area}_{\text{source}}$ (m^2)	5000	12,500 *	20,000	Minimum/maximum estimates from site practices and distribution of organic chemicals manufacture/storage
Phenol, C (mg l^{-1})	7981	10,245 *	12,509	Minimum value obtained from most recent groundwater survey; maximum value is upper limit in source area borehole, 1993–1994.
o-cresol, C (mg l^{-1})	3869	4196 *	4524	Value obtained from most recent groundwater survey
m- and *p*-cresol, C (mg l^{-1})	3382	4409 *	5436	Value obtained from most recent groundwater survey
2,6-xylenol, C (mg l^{-1})	182	251 *	320	Value obtained from most recent groundwater survey
2,4- and 2,5-xylenol, C (mg l^{-1})	1341	1341	1341	Value obtained from most recent groundwater survey
2,3- and 3,5-xylenol, C (mg l^{-1})	496	496	496	Value obtained from most recent groundwater survey
3,4-xylenol, C (mg l^{-1})	220	220	220	Value obtained from most recent groundwater survey
SO_4, C (mg l^{-1})	294	372 *	449	Value obtained from most recent groundwater survey
Reference time, *T* (year)	47	47	47	Age of plume based on site history and practices.
Infiltration, *I* (m year^{-1})	0.1	0.21 *	0.32	Lowest value accounts for made ground and highest value is UK Environment Agency estimate.
Plume residuals				
Phenol (g)	NA	1.04E + 09	NA	Calculated from groundwater quality data and plume dimensions
o-cresol (g)	NA	4.94E + 08	NA	Calculated from groundwater quality data and plume dimensions
m- and *p*-cresol (g)	NA	3.77E + 08	NA	Calculated from groundwater quality data and plume dimensions
2,6-xylenol (g)	NA	1.09E + 08	NA	Calculated from groundwater quality data and plume dimensions
2,4- and 2,5-xylenol (g)	NA	1.05E + 08	NA	Calculated from groundwater quality data and plume dimensions
2,3- and 3,5-xylenol (g)	NA	6.63E + 07	NA	Calculated from groundwater quality data and plume dimensions

Table 5 (*continued*)

Parameter	Value			Comments
	Minimum	Likely	Maximum	
Plume residuals				
3,4-xylenol (g)	NA	1.94E+07	NA	Calculated from groundwater quality data and plume dimensions
SO_4 (g)	NA	7.52E+07	NA	Calculated from groundwater quality data and plume dimensions
Mn (g)	NA	4.14E+06	NA	Calculated from groundwater quality data and plume dimensions
Fe (g)	NA	4.85E+06	NA	Calculated from groundwater quality data and plume dimensions
TDIC–CO_2 (g)	NA	1.03E+08	NA	Calculated from groundwater quality data and plume dimensions
TDIC–CH_4 (g)	NA	1.18E+06	NA	Calculated from groundwater quality data and plume dimensions
Background groundwater				
O_2, C (mg l^{-1})	0	2	12	Value obtained from most recent groundwater survey
NO_3, C (mg l^{-1})	22.3	27.2 *	32.1	Value obtained from most recent groundwater survey
SO_4, C (mg l^{-1})	65.4	79.3 *	93.1	Value obtained from most recent groundwater survey
TDIC, C (mg l^{-1})	30	30	30	Value obtained from most recent groundwater survey
Aquifer hydrogeology				
K_h (m day^{-1})	0.3	0.55 *	0.8	Values obtained from aquifer pumping tests (Aspinwall and Co.)
K_x	0.003	0.005 *	0.007	Values obtained from aquifer pumping tests (Aspinwall and Co.)
Porosity, n_e	0.25	0.265 *	0.28	Total porosity obtained from core analysis (Aspinwall and Co.)
α_y (m)	3.3	3.3	3.3	Calibration of analytical transport model using groundwater Cl concentration in plume (J. Alexander, pers. com.)
α_z (m)	0.5	0.5	0.5	Calibration of analytical transport model using groundwater Cl concentration in plume (J. Alexander, pers. com.)
δy (m)	0.1	2.9	5.7	Thickness of mixing zone obtained from vertical solute profiles using nested piezometer positioned along plume flowpath

Vel_x: Horizontal average linear velocity; α_y: horizontal transverse dispersivity; α_z: vertical transverse dispersivity; TDIC: total inorganic carbon; * mean value of range given; TDIC–CO_2, TDIC–CH_4: total dissolved inorganic carbon calculated from dissolved CO_2 concentrations and dissolved CH_4 concentrations.

dispersivity), or where the use of a range is inappropriate (e.g. plume dimensions and reference time).

4.4. Plume source term inputs

A relatively wide range in values for A_{source} and infiltration were used in the models, in the absence of detailed information on spill areas. These are estimates based on known site practices and are taken from the consultants' site investigation (J. Alexander, 1996, pers. com.). The organic inputs are constant for each scenario tested, with the exception of phenol, cresols and 2,6-xylenol. The range included for these compounds reflects that measured over a 3-year interval in a nested piezometer, located at shallow depth in the plume source area (Fig. 2). Only one analysis is available for the other organic compounds in this borehole and therefore this single value is used as the model input. Sulphate concentrations in the plume, arising from spillage of mineral acids, are generally higher than that in the uncontaminated groundwater. The SO_4 inputs for the model are the range between the maximum concentration measured in the plume (449 mg l^{-1}) and the source area borehole. This assumes that SO_4 concentrations of at least the maximum value found in the plume have originated from the source area. The calculations are performed for a time scale of 47 years, representing the period of groundwater contamination up until the most recent groundwater quality surveys (1997).

4.5. Background groundwater inputs

The calculation of EA inputs from advection of background groundwater into the rear of the plume assumes that the plume extends to full depth in the vicinity of source area. Values of n_k were obtained from analyses of rock cores (Aspinwall and Co., 1992). Values of vel_x were computed from ranges of aquifer horizontal hydraulic conductivity (K_h) and hydraulic gradient (I_h), which were obtained from pumping test data for boreholes in the plume. These agree with the overall migration of the plume. Concentrations of O_2, NO_3 and SO_4 in samples from an uncontaminated borehole upsteam of the site were used to calculate the input of soluble EA from the background groundwater. Sulphate is included in the calculations to account for contributions where the mean concentration of SO_4 in the plume is less than the uncontaminated groundwater. The concentration of TDIC in the background groundwater is also used to calculate the input for correction of the plume residual TDIC fraction (see below).

4.6. Horizontal transverse inputs

The input of aqueous EA to the plume from the background groundwater, by horizontal transverse dispersion at the plume fringe, is estimated from Fick's Law. A value of α_y was estimated as $\alpha_x/3$ (Gelhar et al., 1992), where α_x is the longitudinal dispersivity of the plume (10 m), obtained from transport modelling of the Cl plume at the site (J. Alexander, 1996, pers. com.). A value of δC (mg l^{-1}) is obtained from the difference between the mean concentration of soluble EA in the uncontaminated groundwater and the plume, and δy is the thickness of the mixing zone at the plume fringe (m). Inputs of SO_4 were calculated for the sectional area of the plume where concentrations were below background levels (93 mg l^{-1}). Values of δy were estimated from Cl profiles obtained from a nested piezometer borehole. There is likely to be considerable uncertainty in the value of δy due to the coarse resolution of the plume fringe provided by the vertical spacing of the piezometer wells. The maximum value (5.7 m) was therefore used as input in the reference case and a value of 0.1 m was included as the expected minimum for δy in the Monte Carlo simulations, to assess the effect of uncertainty in this parameter.

4.7. Vertical transverse inputs

A value of α_z for the plume was obtained from transport modelling of the Cl plume, as $\alpha_x/20$ (Gelhar et al., 1992). The solute concentration gradient at the plume margin ($\delta C/\delta y$) was the same as that used to calculate the horizontal transverse dispersive input. The calculated vertical transverse input was doubled to account for contributions from the upper and lower faces of the plume.

4.8. Plume residual inputs

The input of residual organic and inorganic fractions in the box model was estimated by the integration of the contoured solute concentration plots, using the volume of aquifer contained within a contoured interval and the mean solute concentration within that interval. This mass was obtained for each species using concentrations and aquifer volume bounded by the contoured solute concentration plots derived from the groundwater quality surveys and computer modelling. The accuracy of this calculation was tested in the Monte Carlo analyses by assigning different probability distributions to the solute concentration range bounded by each contour.

The residual fractions in the plume comprise non-degraded contaminants, products of reduced EA (Mn^{2+}, Fe^{2+}, S^{2-}) and degradation products (CO_2 and CH_4). Concentrations of Mn^{2+} and Fe^{2+} provide an estimate of the fraction of aquifer mineral oxidants consumed by degradation in the plume. Two estimates of the contribution of Fe mineral oxidants in the plume EA budget were obtained from the available data. These comprised a lower estimate, based on the mass of dissolved Fe^{2+} in the plume, and an upper value obtained from the estimated amount of SO_4-reduction. The calculation of the upper estimate assumes that all S^{2-} produced from SO_4-reduction reacts with soluble Fe^{2+} and is precipitated as insoluble FeS on the aquifer solids. The additional fraction attributed to SO_4-reduction can be combined with the fraction derived from the dissolved Fe^{2+} concentration, to provide a maximum mass of Fe mineral oxidant consumption for the plume.

The TDIC produced as metabolites in the plume is corrected to account for the background level of TDIC (Table 5). The concentrations of residual organic and inorganic solutes in the plume are the same for each scenario tested but the final masses differ based on the value of n_k used in the calculations. A correction of the estimated mass of organic ED consumed may be required to account for background levels of total organic carbon (TOC) in the plume. This was not necessary for this plume as background groundwater TOC concentrations were below detection limits.

4.9. Model scenarios evaluated

Four model scenarios were tested using an identical conceptual model of the plume processes, but different assumed ranges of parameter inputs. The standard model (model A) used the most likely value of each input parameter. An exception was made for δy in this model, where the maximum field estimate (5.7 m) was used, since the most likely value was unknown. In the other models (B, C, D), different probability distributions were assigned to the input parameters (based on the available data), which were then sampled by Monte Carlo analysis to produce a range in forecast outputs. The outputs from the models were compared to understand the effects of uncertainty in the input parameters and to identify the most sensitive inputs in the box model predictions. The parameter values and probability distributions assigned to each model scenario are shown in Table 6.

In model B, the input parameters were assigned a uniform probability distribution, using the minimum and maximum values in each range as limits (Table 5). This distribution assumes that all parameter values between the limits occur with equal chance, and is appropriate where no information exists on the most likely value of a limited range of measurements (Jefferies et al., 1993). In model C, the input parameters are assigned a triangular probability distribution, using minimum, likely and maximum values for the ranges available (Table 5). Triangular probability distributions are useful for describing variability in parameters in complex systems composed of many elements (Hass et al., 1996; Jefferies et al., 1993). The most likely value of a given parameter is expected to fall between the limits of the distribution, but its position may reflect the mean of a relatively restricted range of measurements or a typical analysis within a fixed range (e.g. background concentrations of dissolved oxygen). In model D, the probability distributions were modified to include additional information for some parameters. The modifications were made using data obtained from the site investigation study only, and not by the addition of assumed parameter values or information from literature sources.

Lognormal distributions were assigned to the background groundwater concentration of NO_3 and SO_4, using values for mean and standard deviation calculated from the two groundwater quality surveys. The range for each oxidant is extended to zero and also truncated at the maximum concentration measured in the groundwater. Extending these distributions to zero reflects the case where these oxidants are depleted in uncontaminated groundwater prior to mixing with the plume. This can arise due to the utilisation in the aquifer above the plume, caused by organic loadings from arable farming activities in the overlying field. The use of lognormal probability distributions is acceptable for parameter values which may be skewed but cannot fall below zero (Decisioneering, 1996). This probability distribution has been used to describe parameter uncertainty in hydrogeological properties in other studies (Goodrich and McCord, 1995; McNab and Dooher, 1998). It is not possible to assign a similar distribution to the background concentration of dissolved oxygen as only one measurement is available. However, theoretical upper and lower limits, which may occur in the distribution for this oxidant, are included in the analysis (Table 5). The value of hydraulic conductivity (K_h) used in models A, B and C is a range, which is averaged over the depth of the aquifer. This range was improved for model D by including the values of K_h determined for each monitoring borehole in the plume. A logistic distribution was obtained for this new data using the best-fit distribution option in Crystal Ball®

Table 6
Parameter values and probability distributions used in different model scenarios

Parameter	Value or distribution			
	Model A	Model B	Model C	Model D
Plume dimensions				
Width (m)	131	131	131	131
Length (m)	525	525	525	525
Depth (m)	40	40	40	40
Plume source strengths				
Phenol, C (mg l^{-1})	10,245	*U*	*T*	*T*
o-cresol, C (mg l^{-1})	4196	*U*	*T*	*T*
m- and *p*-cresol, C (mg l^{-1})	4409	*U*	*T*	*T*
2,6-xylenol, C (mg l^{-1})	251	*U*	*T*	*T*
2,4- and 2,5-xylenol, C (mg l^{-1})	1341	1341	1341	1341
2,3- and 3,5-xylenol, C (mg l^{-1})	496	496	496	496
3,4-xylenol, C (mg l^{-1})	220	220	220	220
SO_4, C (mg l^{-1})	305	*U*	*T*	*T*
Reference time, *T* (year)	47	47	47	47
Infiltration, *I* (m year^{-1})	0.21	*U*	*T*	*T*
Plume residuals				
Phenol (g)	1.04E+09	*U*	*T*	*T*
o-cresol (g)	4.94E+08	*U*	*T*	*T*
m- and *p*-cresol (g)	3.77E+08	*U*	*T*	*T*
2,6-xylenol (g)	1.09E+08	*U*	*T*	*T*
2,4- and 2,5-xylenol (g)	1.05E+08	*U*	*T*	*T*
2,3- and 3,5-xylenol (g)	6.63E+07	*U*	*T*	*T*
3,4-xylenol (g)	1.94E+07	*U*	*T*	*T*
SO_4 (g)	7.52E+07	*U*	*T*	*T*
Mn (g)	4.14E+06	*U*	*T*	*T*
Fe (g)	4.85E+06	*U*	*T*	*T*
$\mathrm{TDIC}_{\mathrm{carbon\ dioxide}}$ (g)	1.03E+08	*U*	*T*	*T*
$\mathrm{TDIC}_{\mathrm{methane}}$ (g)	1.18E+06	*U*	*T*	*T*
Background groundwater				
O_2, C (mg l^{-1})	2	*U*	*T*	*T*
NO_3, C (mg l^{-1})	27.2	*U*	*T*	LN (27.21 ± 2.72, 0-32.1)
SO_4, C (mg l^{-1})	79.3	*U*	*T*	LN (79.25 ± 7.93, 0-93.1)
TDIC, C (mg l^{-1})	30	30	30	30
Aquifer hydrogeology				
K_x (m day^{-1})	0.55	*U*	*T*	LG (0.84, 0.15)
I_x	0.005	*U*	*T*	*T*
Porosity, n_e	0.26	*U*	*T*	*N* (0.26 ± 0.03)
α_y (m)	3.3	3.3	3.3	3.3
α_z (m)	0.5	0.5	0.5	0.5
δy (m)	5.7	*U*	*T*	*T*

Notes: *U*: Uniform distribution; *T*: Triangular distribution; *N*: Normal distribution (mean ± standard deviation); LN: lognormal distribution (mean ± standard deviation, selected range); LG: logistic distribution (mean, scale value).

(Decisioneering, 1996). A normal distribution was also assigned to the aquifer porosity in this model, as has been used in similar studies elsewhere (McNab and Dooher, 1998).

5. Results

5.1. Model outputs

Calculated electron and carbon balances for the different models are shown in electron equivalents ($e^- \times 10^5$) in Table 7. Forecasts are presented for the plume source and EA inputs, plume residuals, degradation products and plume balance in each model. Mean values and the output range between the 95% confidence level are presented for each Monte Carlo forecast The results of the standard case (model A) are reviewed below. The results of the Monte Carlo analyses (models B, C and D) are compared in the sensitivity analysis (see below) using model A as the reference case.

5.2. Plume electron donor and electron acceptor inputs and residuals

The plume source inputs comprise EA (SO_4 from mineral acid spills) and ED (phenol, cresols and xylenols). The ED input (organic contaminants) exceeds the EA input by two orders of magnitude. Inputs of aqueous EA into the plume from uncontaminated groundwater include contributions from advection and dispersion. Estimated inputs from these sources are similar. The organic ED and inorganic EA (SO_4) residuals represent the estimated fractions of unconsumed organic contaminants and soluble oxidants, respectively. These are subtracted from the appropriate source term inputs to respectively obtain an estimate of the organic ED and inorganic EA consumed within the plume.

The mass of Fe^{2+} and Mn^{2+} in the plume provides a minimum estimate of the aquifer mineral oxidants consumed by degradation. An estimate of the additional fraction of Fe oxides consumed by degradation can be obtained from the SO_4 balance for the plume. This assumes that the SO_4 deficit is attributable to SO_4-reduction and that the S^{2-} formed removes dissolved Fe^{2+} by precipitation of Fe sulphide phases. The apparent contribution of mineral oxidants in the EA budget for the plume is an order of magnitude less than the soluble EA fractions. Additional contributions corrected for SO_4-reduction are negligible. Analysis of rock core samples from the plume and stable isotopic studies indicate that there is negligible Fe and S present in solid phases and that SO_4-reduction is not significant in the plume (Spence et al., in press). Reactive transport modelling of the plume also showed that the contribution of metal oxide reduction in degradation is small. This was deduced by accounting for SO_4-reduction and fermentation using stable isotope data and CH_4 concentrations, and then using the measured TDIC concentration to constrain the upper limit of Fe and Mn oxide reduction (Mayer et al., submitted for publication).

5.3. Dissolved inorganic carbon

Accumulated products of contaminant degradation in the plume are presented as TDIC. These comprise the sum of CO_2-derived inorganic carbon and equivalent TDIC corre-

Table 7
Summary of electron and carbon balance in different model scenarios ($e^- \times 10^5$)

Forecast	Model A	Model B[a]		Model C[a]		Model D[a]	
		Mean	0.95 level	Mean	0.95 level	Mean	0.95 level
Plume source inputs							
Electron acceptors	38.2	38.4	13.5–90	38.2	19–80	38.2	19.1–80
Electron donors	8040	8069	2890–20,000	8050	4110–15,000	8030	4080–15,000
Electron acceptor inputs from groundwater							
Advection	22.4	23.5	11.3–50	23.2	14.3–40	34.9	15.6–70
Horizontal dispersion	17.1	120	13.7–1500	52.6	18–225	78.6	21.6–350
Vertical dispersion	22.4	152	17.6–1750	67.5	23.4–300	100	28–500
Plume residuals							
Electron acceptors (Fe^{2+} and Mn^{2+})	2.37	2.37	2.01–2.78	2.37	2.11–2.67	2.38	1.86–2.93
Electron donors	6832	6820	6100–7560	6820	6320–7350	6840	5630–8080
Fe oxide consumed from SO_4 lost[b]	0.42	7.79	− 2.73–100	3.0	− 1.45–17.5	5.99	− 0.89–30
Degradation products							
Total inorganic carbon	348	348	248–451	349	276–422	349	260–445
Plume balance							
Net electron acceptor consumption[c]	39.7	284	14.5–852	119	30.2–288	191	42.6–467
Net electron donor consumption	1208	1240	− 3950–12,500	1210	− 2760–10,000	1190	− 2900–10,000
Difference between TDIC produced and EA consumption[d]	308	56	− 546–389	227	39.5–356	152	− 140–351
Estimated source term[e]	7180	7170	6440–7930	7170	6650–7000	7190	5910–8480

[a] Forecasts from Monte Carlo analyses.

[b] Stoichiometric quantity of additional FeOOH consumed by precipitation of FeS, based on net consumption of SO_4 in plume (see text).

[c] Uncorrected for additional estimated loss of solid phase Fe obtained from net SO_4 consumption in plume.

[d] Value includes correction for additional electron acceptor loss due to estimated solid phase Fe consumption calculated from net SO_4 lost.

[e] Sum of plume electron donor and TDIC residuals.

sponding to the mass of CH_4 produced. The net TDIC production in the plume is an order of magnitude higher than the combined EA inputs.

5.4. Plume balance

Estimates of the net EA consumption for the plume are obtained from the difference between total input and plume residual EA fractions. The contribution of mineral oxidant consumption is obtained from the dissolved Fe and Mn fractions in the plume, but this does not include the potential mass attributable to SO_4-reduction. The latter can only be obtained indirectly and its omission does not significantly affect the overall EA budget. Estimates of net ED consumption are obtained from the difference between the source input and plume residual ED fractions. This estimate is two orders of magnitude higher than the estimated EA consumption. The balance between TDIC production in the plume and EA consumption suggests that there is an excess of TDIC in the plume over that explained by the estimated EA consumption.

The plume source term can be estimated by the summation of the residual ED fraction and TDIC produced in the plume. This assumes that the TDIC originates from organic contaminant degradation over the history of the plume. The evidence supporting this assumption is discussed below.

5.5. Specific electron acceptor consumption

The contribution of each oxidant in the budget of EA consumed within the plume (Table 6) is presented in Table 8. The consumption of CO_2 via CH_4 generation is also included for comparison, but it is not part of the estimated net EA consumption (Table 6), since CO_2 is produced from degradation processes within the plume. The general sequence of oxidant consumption for the standard model (A), in order of decreasing importance, is:

$$\mathrm{NO_3} > \mathrm{CO_2} > \mathrm{O_2} > \mathrm{SO_4} > \text{Mn oxides} > \text{Fe oxides}$$

From the data in Table 8, aerobic degradation and NO_3-reduction are quantitatively more important than all other processes combined. The contribution of SO_4-reduction, using SO_4 supplied via the plume source or uncontaminated groundwater, cannot be determined with accuracy using the available data (see below). Contaminant degradation using aquifer Mn and Fe oxides is occurring throughout the plume, but the contribution of these processes in the EA budget is very small.

5.6. Sensitivity analyses

The sensitivity analyses compare the importance of the probability distribution functions assigned to each input parameter in models B, C and D and identify the critical inputs that introduce the greatest uncertainty in performance predictions obtained with the box model. These effects are reviewed in turn below.

Table 8
Summary of estimated oxidant consumption for models ($e^- \times 10^5$)

Oxidant	Model A	Model B		Model C		Model D	
		Mean	0.95 level	Mean	0.95 level	Mean	0.95 level
O_2	3.47	53.8	1.7–159	19.6	2.83–51.9	29.7	3.69–82.5
NO_3	30.5	163	20.8–483	73.7	28.2–171	111	32.8–265
SO_4	3.36	64.8	− 21.8–219	23.4	− 12.4–73.5	48	− 7.1–129
CO_2	7.89	7.91	2.91–13	7.87	4.11–11.7	7.89	4.03–12
Mn	1.51	1.51	1.23–1.79	1.5	1.31–1.71	1.51	1.2–1.83
Fe	0.86	0.86	0.71–1.02	0.86	0.76–0.97	0.86	0.69–1.05
Total[a]	39.7	284		119		191	

[a] Excludes CO_2.

5.6.1. *Effect of probability distribution*

The effects of probability distributions assigned to parameter inputs for the box model on the resulting Monte Carlo forecasts are compared with the standard model (A) in Table 9. Generally, greater variation in forecasts was obtained when a uniform probability distribution was used for parameter inputs (model B). However, the forecast mean estimates obtained in the Monte Carlo simulations are consistent and similar to those obtained with the standard model. Negative values are obtained for some forecasts, at the 95% confidence level. For the contribution of Fe oxide consumption estimated from SO_4-reduction, a negative value occurs when the estimated SO_4 input (from the plume source and background groundwater) is less than the residual SO_4 fraction. The latter is similar for each model and always positive (data not shown), so the range in this estimate reflects the uncertainty in the other SO_4 inputs. Similarly, a negative balance for the net ED consumption reflects the uncertainty in the estimate of the source ED input, rather than the plume residual ED fraction. Negative forecasts of the difference between TDIC production in the plume and estimated EA consumption indicate that the EA consumption can exceed the TDIC production. The reasons for this are discussed below.

5.6.2. *Effects of parameter uncertainty on model predictions*

Sensitivity analyses were completed for each Monte Carlo forecast to identify which input parameters create the greatest uncertainty in the box model predictions. In turn, this targets input parameters or properties, which need greater characterisation during a site investigation prior to performance assessment of NA using the box model. Results of the sensitivity analyses for selected model forecasts are summarised in Table 10. The percentage of variance contributed by each parameter in the Monte Carlo forecasts is also shown. These percentages represent the maximum values obtained in either models B, C or D. This information identifies the most sensitive and least sensitive parameters of forecasts used to define the key outputs of the box model and the plume status. An example output of a typical sensitivity analysis is shown in Fig. 5.

Source area and infiltration primarily account for uncertainty in forecasts of the plume source ED input (Table 10). Contaminant concentration has a negligible effect (2%) on the predicted organic source term. This forecast is also insensitive to the probability

Table 9
Effect of parameter probability distribution function on Monte Carlo forecasts for the box model

Forecast	Effect of probability distribution in models B, C and D compared with base case (model A)
Plume source inputs	Mean ED input is similar but range in models B, C and D varies by up to a factor of seven. Mean EA inputs are similar with variation over a relatively narrow range.
Aqueous EA inputs	Inputs from advection are similar but inputs from dispersion vary over a wide range and are up to two orders of magnitude higher, with greatest variation for a uniform distribution (model B).
Plume residuals	Mean mineral oxidant inputs and ED residuals are similar and vary over a narrow range. Mean estimates of mineral oxide consumption based on SO_4-reduction are an order of magnitude higher, with a range that varies by up to three orders of magnitude, and which may be negative.
Degradation products	Mean inputs of TIC are similar with variation by less than a factor of two.
Plume balance	Mean estimates of net EA consumption are higher by an order of magnitude but the range includes value of base case. Mean estimates of net ED consumption are similar but the range varies by up to a factor of four and may be negative. Mean estimates of the difference between TIC production and EA consumption vary by one order of magnitude, and have a balance which may be negative but which includes the estimates from the base case. Mean estimates of the plume source term are similar.

distribution assigned to each parameter. Estimates of the plume ED consumption are primarily sensitive to the source area and infiltration terms used. The probability distribution assigned to each parameter has no significant effect on this forecast.

Estimates of EA inputs to the plume from dispersion are primarily dependent on the transverse mixing zone width, δy. Variation in aquifer hydraulic conductivity and hydraulic gradient is less important, and the background aqueous oxidant concentrations have no significant effect on the forecasts. The assumption of a normal probability distribution for n_k in model D increases the uncertainty in the forecast from this parameter, but δy remains the critical input. The net EA consumption in the plume is also primarily controlled by δy (Fig. 5). This result occurs because the plume EA consumption is the balance between all inputs (background groundwater, source area) and the plume residuals. Although the source area EA input may be high (Table 7), estimates of net consumption are affected more by uncertainty in the aquifer hydrogeological properties than source area characteristics.

Estimates of the TDIC fraction in the plume are primarily influenced by the calculated mass of inorganic carbon (CO_2), rather than aquifer porosity or the mass of CH_4. Uncertainty in the value of aquifer porosity accounts for more variability in the TDIC estimate in model D, although this does not change the mean forecast, which is the same for all models (Table 7). Also, uncertainty in both parameters has no significant effect on the mean value of the mass estimates, regardless of the probability distribution used. A similar result was obtained for estimates of the plume ED residuals (data not shown). Accurate sampling and analysis of dissolved inorganic carbon and contaminant fractions is

Table 10
Summary of parameter sensitivity in selected forecasts for plume box model

Forecast	Most sensitive input parameter	Least sensitive input parameter
Plume source input	Source area (57%), infiltration (41%)	Source organic contaminant concentration (2%)
Plume ED consumption	Source area (57%), infiltration (40%)	Source organic contaminant concentration, aquifer porosity, plume residual organic contaminant mass (total of 3%)
EA inputs from dispersion	Transverse mixing zone width (76%)	Aquifer hydraulic conductivity (12%), hydraulic gradient (9%), background groundwater oxidant concentration (2.5%)
Plume EA consumption	Transverse mixing zone width (48%), aquifer hydraulic conductivity (37%)	Aquifer hydraulic gradient (10%), background groundwater oxidant concentration, source area, infiltration (others total 5%)
Degradation product, as TDIC	Dissolved CO_2 mass (97%)	Aquifer porosity, CH_4-derived TIC (3%)
Balance between TDIC production and EA consumption	Transverse mixing zone width (51%), dissolved CO_2 mass (35%)	Aquifer porosity, background groundwater oxidant concentration, source area, infiltration (total 14%)

Note: Percentage of forecast variance contributed by individual parameters is shown in parentheses.

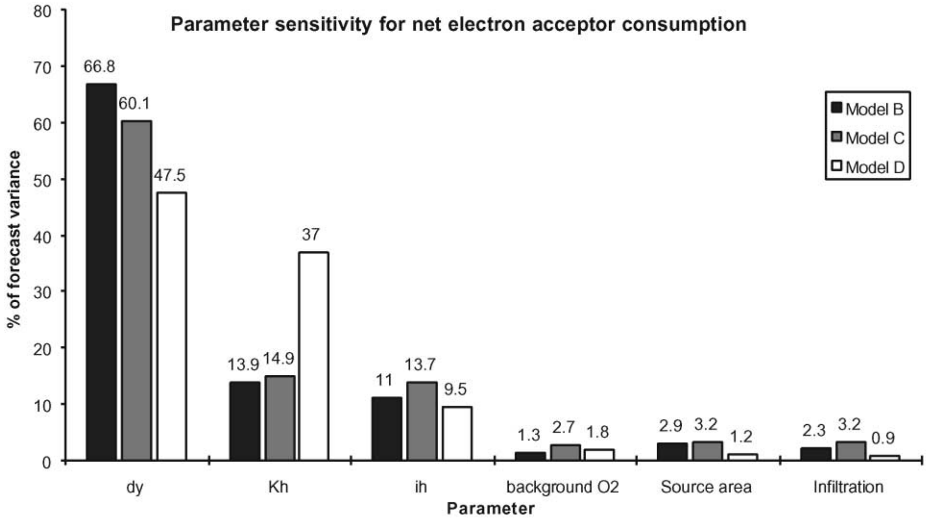

Fig. 5. Parameter sensitivity for electron acceptor consumption predicted by the Monte Carlo simulations (percentage of forecast variance is shown above each block).

therefore more important than the aquifer properties to obtain a reliable estimate of these inputs. The balance between the TDIC residual and EA consumption is most sensitive to δy and the calculated mass of dissolved CO_2 (Table 10).

Forecast estimates of aqueous EA (O_2, NO_3, SO_4) consumption in models B, C and D are higher than that obtained using fixed parameter inputs in model A (Table 8). The forecast range for these species at the 95% confidence interval is also larger than that for the mineral oxidants or CO_2 in each model, due to uncertainty in the value of δy. Negative values of SO_4 consumption occur in the Monte Carlo analyses. This is because of uncertainty in the source spill area for this EA input, which may be underestimated compared with the other EA inputs. This indicates that loss of SO_4 in this plume may not be statistically identified from the data.

The average and maximum range of the mean estimate of each oxidant consumed in models B to D is: O_2: 27.5 tonnes (1.4–127); NO_3: 144 tonnes (25.8–599); CO_2: 4.3 tonnes (1.6–7.2); MnO_2: 6.5 tonnes (5.2–7.9); FeOOH: 7.6 tonnes (6.1–9.3). The mean contaminant mass loss (as TOC) attributable to consumption of these oxidants is: O_2: 10.3 tonnes; NO_3: 34.8 tonnes; CO_2: 1.2 tonnes; MnO_2: 0.45 tonnes; FeOOH: 0.26 tonnes. If consumption of SO_4 is occurring, the average of the mean loss predicted by models B to D is 54 tonnes, with a maximum loss of 263 tonnes. This would account for a mean contaminant mass loss attributable to SO_4-reduction of 13.5 tonnes TOC. Because O_2 and NO_3 are only supplied from the uncontaminated groundwater via dispersive mixing, the results suggest that the degradation potential is greatest at the plume fringe. In contrast, the contribution of mineral oxidant reduction and methanogenesis in mass turnover throughout the plume is very low.

6. Discussion

6.1. Sensitivity of plume box model to probability distributions of input parameters

The plume box model was tested using a range of assumed probability distributions for the parameter inputs. In general a uniform distribution produced the greatest variance in the model forecasts. Triangular probability distributions are often used in environmental performance assessments when little information on parameter distributions is available or as part of a first-pass analysis (Jefferies et al., 1993). Results using triangular probability distributions for parameter inputs were generally similar to that of model D, in which empirically determined probability distributions obtained from fitting distributions to the site data were also used for some parameters (e.g. aquifer hydraulic conductivity). The results suggest that the selection of triangular probability distributions as a default for parameter inputs in the box model will be adequate, avoiding the need for greater characterisation (i.e. increased sampling) of parameter uncertainty. However, as demonstrated by the results from models B and C, it is important to compare the effects of different probability assumptions on the forecast values, to properly understand the variance introduced in the model predictions for identical parameter inputs.

6.2. Estimates of contaminant source term and mass loss

The average of the mean value of the ED source input from all models is 8.047×10^8 e^-, equivalent to 2414 tonnes of contaminant carbon (as TOC). The maximum range in this input is 867 to 6000 tonnes TOC (model D). The average mean residual ED fraction in the plume is 2048 tonnes TOC, with a maximum range of 1689 to 2409 tonnes TOC. This provides a mean contaminant loss of 366 tonnes TOC over the history of the plume. The Monte Carlo analyses indicate that a negative forecast can be obtained for this estimate due to uncertainty in the source term. This uncertainty arises primarily from inadequate understanding of the source area, and in particular the underestimation of this parameter at the lower end of the range used in the models. Estimates of the plume source term input are most sensitive to variations in spill area (and infiltration), rather than the source strength (contaminant concentration). This information can only usually be acquired from a site audit of spillages, site practices and/or investigation of contaminant distribution in the source zone. However, estimates so obtained may still be associated with considerable uncertainty in the model. The site records do not allow a reliable determination of the plume source term to be made for the plume under study. Accurate estimates of contaminant mass loss cannot therefore be obtained from the balance between the plume ED source term and residual fraction.

The TDIC produced within the plume may be derived from degradation processes or interaction with carbonate minerals or a combination of both. Geochemical modelling of the hydrochemical data using MINTEQA2 (Allison et al., 1990) indicates that both the background and contaminated groundwater in the aquifer are undersaturated with respect to carbonate minerals (saturation indices < 0.0), to a depth of 50 m below ground level (Table 11). This suggests that there are no detrital or authigenic carbonates, which may influence the groundwater TDIC concentration in this section of the aquifer. However,

Table 11
Modelled saturation indices (SI) for groundwater samples

BH	Carbonates					Sulphates		Sulphides			
	Calcite	Aragonite	Dolomite	Siderite	Rhodocrosite	Anhydrite	Gypsum	FeSppt	Mackinawite	Pyrite	Sulphur
3d	−3.89	−4.09	−7.81	−4.59	−4.21	−2.11	−1.73	−5.8	−5.07	22.45	15.12
8d	−2.74	−2.94	−6.08	−2.17	−2.36	−1.54	−1.17	−3.77	−3.03	14.38	5.08
9m	1.39	1.2	1.78	3.03	1.02	−2.64	−2.29	2.25	2.98	28.54	13.28
9d	−1.51	−1.71	−3.27	−1.15	−0.83	−2.47	−2.12	−2.58	−1.85	19.78	9.35
13	0.07	−0.06	−1.36	−1.15	−0.36	−1.31	−1.1	−0.57	0.15	25.94	14.07
14	−1.84	−2.04	−4.41	−1.39	−1.19	−1.37	−1.01	−2.58	−1.85	20.21	9.73
15	−2.56	−2.77	−5.52	−1.32	−1.95	−2.12	−1.73	−3.25	−2.52	16.75	6.85
40	−1.32	−1.53	−3.18	−0.36	−0.53	−0.91	−0.51	−2.72	−1.99	15.85	5.4
41	−3.61	−3.81	−7.75	−4.94	−4.46	−1.56	−1.18	−5.98	−5.24	18.63	11.48
43	−0.15	−0.35	−1.66	−0.08	0.17	−1.61	−1.23	−1.28	−0.55	12.57	0.76
44	−0.11	−0.31	−1.73	−0.11	−0.51	−1.49	−1.12	0.22	0.95	20.67	7.34
48	−0.19	−0.41	−1.37	−1.03	−0.96	−2.55	−2.15	0.72	1.45	17.59	3.67
55	−1.94	−2.16	−4.43	−1.62	−1.34	−1.33	−0.95	−3.2	−2.46	11.88	1.98
57	−0.85	−1.06	−2.92	−2.4	−1.66	−1.43	−1.05	NA	NA	NA	NA

Notes: Mineral formulas are: calcite, aragonite: $CaCO_3$; dolomite: $(CaMg\,(CO_3)_2)$; siderite: $FeCO_3$; rhodocrosite: $MnCO_3$; anhydrite: $CaSO_4$; gypsum: $CaSO_4 \cdot 2H_2O$; mackinawite: FeS; pyrite: FeS_2; sulphur: S^0.

Mineral phases are undersaturated in groundwater when $SI < 0.0$, in equilibrium when $SI = 0.0$ and oversaturated when $SI > 0.0$.

NA = Not available due to Fe^{2+} below detection limits.

stable isotope analysis of the plume TDIC indicates that it is derived from the degradation of the organic contaminants (80%) and dissolution of sedimentary carbonate (20%) (Thornton et al., 2001). This explains the geochemical modelling results, which indicate that sedimentary carbonates are not currently present in the plume section. There are two monitoring boreholes which are an exception. These are BH9m and BH13. At the former location, the groundwater is oversaturated with respect to $CaCO_3$, $FeCO_3$ and $MnCO_3$ phases, implying that these may precipitate to reduce the TDIC. This condition is due to a shallow NaOH plume close to the site, which raises the alkalinity of the groundwater (Williams et al., 2001). However, no carbonate phases were detected by analysis of rock core samples from within the NaOH plume (Spence et al., 2001), suggesting that loss of TDIC by this mechanism is not occurring. The calcite equilibrium predicted for groundwater from BH13 may arise from the production of inorganic alkalinity caused by SO_4-reduction, which is active at this location (Williams et al., 2001). Additional hydrochemical modelling using the PHREEQM code (Appelo and Postma, 1993) suggests that the plume is also physically closed with respect to loss of dissolved CO_2. These results imply that the excess TDIC derived from degradation is conserved within the system. The ED consumption can therefore be constrained by the TDIC fraction, by assuming that this records the amount of contaminants degraded over the history of the plume, after correction for additions from sedimentary carbonate dissolution (Hess et al., 1996). The TDIC in the plume is equivalent to the degradation of 104 tonnes TOC, with a maximum range of 74–135 tonnes. The equivalent TOC corrected for the TDIC contribution from sedimentary carbonate dissolution (20%) is 83.2 tonnes. When added to the plume residual TOC (see above), this provides an estimated source term of 2131 tonnes TOC, with a range of 1748 to 2517 tonnes. This is a conservative estimate as it is based on the TDIC fraction, which is assumed to be conserved within the system and to represent the degradation products over the history of the plume. The TDIC fraction corresponds to degradation of only 4% of this source term (2131 tonnes), much less than the value of 15% estimated from the difference between the ED source input and plume residual. The degradation attributable to the TDIC reservoir corresponds to a mean first order half-life of 819 years (range 743–949 years) for the plume. This half-life is an estimate averaged over the history, volume and range of processes in the plume. The rate does not take into account the higher degradation expected at the plume fringe (note the high NO_3 consumption in electron balance). Also, the rate may not be applicable in the future. For example, most of the degradation in the plume may have occurred in recent decades. The current low mass loss may not be representative of conditions in the uncontaminated aquifer after increased dilution of the plume. However, the estimated half-life has value in illustrating that the plume is likely to be long-lived under the present conditions.

6.3. Plume electron acceptor consumption and budget

The ED consumption estimated from the contaminant source term and residual mass in the plume exceeds EA consumption by up to three orders of magnitude. This difference reflects greater uncertainty in estimating the source term rather than the oxidant consumption, as shown by the forecast ranges for these inputs (Table 7). It is likely that the ED source term has been overestimated. The order of EA consumption in the standard model and that forecast in the Monte Carlo analyses is consistent. This order is considered to represent the relative significance of the degradation processes in contaminant turnover, with NO_3-reduction and aerobic processes occurring at the plume fringe being the most important. Degradation coupled to the reduction of the mineral oxidants is quantitatively insignificant compared with the former two processes. The CO_2 consumed by methanogenesis must be considered a maximum, since it is assumed that CH_4 in the plume arises from the reduction of CO_2, rather than the fermentation of organic compounds. The latter is not explicitly accounted for in the model calculations. However, the contribution of methanogenesis to contaminant turnover, based on CO_2-reduction in the EA budget, appears to be small.

Mineral oxidants are an important source of EA for biodegradation in polluted aquifers (Christensen et al., 1994; Cozzarelli et al., 1995; Heron and Christensen, 1995), and the microbially catalysed reduction of aquifer Fe oxides is coupled to the oxidation of a wide variety of organic chemicals (Baedecker et al., 1993; Chapelle, 1993; Tuccillo et al., 1999). However, the estimated mineral oxidant consumption due to contaminant degradation in this plume represents 0.4% of the aquifer oxidation capacity, obtained from analysis or rock core samples. Hence, only a trivial fraction of the available reservoir of the aquifer mineral oxidants has been utilised by biodegradation in the plume. The amount consumed must be considered a “bioavailable” fraction, that is, the fraction presently utilised by the indigenous microbial consortia under the environmental conditions in the plume. Work is presently underway to quantify the bioavailable mineral oxidant fraction in this aquifer and to identify the factors controlling Fe-reduction processes in the plume. The lack of significant mineral oxidant consumption may reflect a mineralogical control or microbial limitation on oxidant bioavailability.

Dispersion and advection provide a greater contribution to the EA budget for the plume than inputs from the source area. Of these, dispersive inputs dominate the plume EA budget. However, predicted inputs from dispersion vary by up to two orders of magnitude (Table 7). Estimates of aqueous EA inputs from dispersion are most sensitive to the plume mixing zone width (δy). The dispersive input is in turn driven by the aquifer transverse dispersivity, α. Values of δy and α can only be crudely determined from the existing monitoring borehole network and transport modelling of the Cl plume, respectively, and may be much less than the figures used in the models (Table 5). Evidence from other studies suggests that solute gradients across plume fringes may be steeper (Christensen et al., 1994) and aquifer dispersivity may be less (Gelhar et al., 1992) than that assumed in the models tested in this study.

6.4. Implications of plume electron and carbon balance

The difference between the TDIC produced in the plume and the net EA consumption is 3×10^7 e^- for model A (standard case), but much less for the mean estimates predicted by the Monte Carlo analyses (Table 7). The contaminant mass loss corresponding to the mean net EA consumption (but excluding SO_4-reduction due to uncertainty in documenting its occurrence statistically) is 47 tonnes of TOC. This differs from the estimate (104 tonnes of TOC) obtained from the TDIC residual in the plume by only a factor of two. This agreement is improved when the corrected estimate of 83 tonnes TOC degraded is considered and suggests that the production of metabolites (TDIC and CH_4) from contaminant degradation is approximately balanced by the consumption of EA in the aquifer. An estimate of contaminant mass loss for this system may therefore be obtained from an electron balance, using the consumption of available oxidants, or a carbon balance, based on direct measurement of dissolved TDIC in the plume. The balance between TDIC production and EA consumption for the Monte Carlo forecasts encompasses the value obtained for the standard case (model A). Negative results for this balance simply reflect forecast values in which net EA consumption may exceed net TDIC production. However, the range is no higher than a factor of three (model D). In all cases, the mean estimate is positive, suggesting that there is more TDIC production than oxidant consumption (Table 6). Possible reasons for this include contributions of TDIC from degradation processes (e.g. fermentation) which are not accounted in the box model and/or underestimation of the EA consumption. Fermentation processes would result in the production of TDIC without consumption of inorganic oxidants. Reactive transport modelling of the plume suggests that up to 80% of the TDIC may originate from prior degradation in the unsaturated zone (Mayer et al., submitted for publication). This means that the TDIC corresponding to degradation in the plume (~ 17 tonnes) would be less than the EA consumption in all cases and even more pessimistic for the performance of NA at the site. Underestimation of the EA consumption can arise from uncertainty in oxidant inputs contributed by dispersion, which can vary by over a factor of 100 for the horizontal component (Table 6). Work is presently underway to understand the contribution of fermentation and role of dispersion in the plume mass balance. Of particular significance is that the residual ED fraction in the plume exceeds the forecast EA consumption within the plume by a factor of 35 (Table 6). This indicates that the current organic pollutant load vastly exceeds the assimilative capacity of the aquifer and that the plume is likely to grow substantially under the present conditions. Although the aquifer is not oxidant limited and the phenolic compounds are biodegradable under the range of redox conditions found in the plume, biodegradation may be limited by the environmental conditions at this site. Possible reasons include toxicity from high contaminant concentrations in much of the plume core and the availability of aqueous EA supplied by dispersion at the plume fringe. Natural attenuation of these contaminants may therefore progress to completion only after sufficient dilution of the plume. This implies that transport processes may have a greater impact on pollutant fate in this system than electron acceptor availability.

7. Conclusions

Plume-scale electron and carbon balances can be undertaken for aquifers contaminated with organic chemicals to assess the potential for NA at field-scale. The box model methodology developed in this study provides a robust and practical framework for calculating site-specific global mass balances for plumes. This can in turn quantify the relative importance of degradation processes, enable estimates to be obtained for plume source terms and contaminant mass loss, predict the status (e.g. shrinking, stable, expanding) of plumes and identify possible limiting environmental controls (e.g. oxidant supply, toxicity effects), which may require consideration in any engineered amendment to

NA. The box model approach requires only basic data obtained during a typical site investigation and groundwater monitoring study for NA schemes, but provides a more comprehensive understanding of contaminant fate and plume behaviour than that which can be presently achieved with existing NA protocols. When combined with an analysis of input data uncertainty the box model is a useful tool, capable of providing a realistic performance assessment for NA technology and quantifying the environmental risks to potential receptors. The methodology addresses the uncertainty in hydrogeological and hydrogeochemical data that are available from site investigations for NA assessments. Estimates obtained with the box model are particularly sensitive to uncertainty in the plume source and dispersive flux. Greater sampling and monitoring efforts should be directed during a site investigation to obtain more information on these terms. Reducing the variability in the data required to estimate these inputs may be achieved by a comprehensive site audit and monitoring borehole design, which provides an improved resolution of the plume fringe. The approach may be limited in cases where TDIC is not conserved or in carbonate aquifers where estimates of the contaminant source term and mass loss may be difficult to obtain due to contributions of TDIC from non-biogenic sources.

Application of the box model at the site under study shows that consumption of EA due to contaminant degradation in the aquifer agrees closely with the production of inorganic carbon, which is conserved in the system. A carbon balance suggests that only 4% mass loss has occurred over the 50-year history of the plume, which has a plume-averaged half-life >800 years under the present conditions. The electron balance suggests that degradation potential and mass loss is much higher at the plume fringe than in the plume core. Degradation at the plume fringe is limited by the supply of aqueous EA provided by dispersion, but in the plume core may be limited by mineral oxidant bioavailability and toxicity effects from high contaminant concentrations. Despite the biodegradable nature of the contaminants and availability of suitable EA in the aquifer, the residual contaminant load in the plume exceeds assimilative capacity of the aquifer under the present conditions. Natural attenuation of the plume is likely to increase only after increased transport in the aquifer.

Acknowledgements

This research was sponsored by the UK Environment Agency and Engineering Physical Sciences Research Council in the project “Predicting the potential for natural attenuation of organic contaminants in groundwater”. The authors gratefully acknowledge the assistance of the site owner, Enviros Aspinwall, and Dames and Moore Ltd. in the completion of this work. The authors also thank two reviewers for their constructive comments, which helped improve the manuscript.

References

Abbaspour, K.C., Schulin, R., van Genuchten, M.Th., Schlappi, E., 1998. Procedures for uncertainty analysis applied to a landfill leachate plume. Ground Water 36, 874–883.

Allison, J.D., Brown, D.S., Novo-Gradac, K.J., 1990. MINTEQA2 Metal Speciation Equilibrium Model for Surface and Groundwater, Version 3.00. Center for Exposure Assessment Modelling, U.S. EPA, Athens, GA, USA, 106 pp.

Appelo, C.A.J., Postma, D., 1993. Geochemistry, Groundwater and Pollution. Balkema, Rotterdam.

Aspinwall and Co., 1992. Site investigation at Synthetic Chemicals, Four Ashes. Phase 6 Groundwater assessment. Unpublished consultants report.

Baedecker, M.J., Cozzarelli, I.M., Eganhouse, R.P., Siegel, D.I., Bennet, P.C., 1993. Crude oil in a shallow sand and gravel aquifer: III. Biogeochemical reactions and mass balance modelling in anoxic groundwater. Appl. Geochem. 8, 569–586.

Buscheck, P.E., O'Reilly, K., 1995. Protocol For Monitoring Intrinsic Bioremediation in Groundwater. Report of Chevron Research and Technology, Chevron, San Francisco, p. 20.

Chapelle, F.H., 1993. Ground-Water Microbiology and Geochemistry. Wiley, New York.

Christensen, T.H., Kjeldsen, P., Albrechtsen, H., Heron, G., Nielsen, P.H., Bjerg, P.L., Holm, P.E., 1994. Attenuation of landfill leachate pollutants in aquifers. Crit. Rev. Environ. Sci. Technol. 24, 119–202.

Cozzarelli, I.M., Herman, J.S., Baedecker, M.J., 1995. Fate of microbial metabolites of hydrocarbons in a Coastal Plain aquifer; the role of electron acceptors. Environ. Sci. Technol. 29, 459–469.

Decisioneering, 1996. Crystal Ball®, version 4, User manual.

Environment Agency, 2000. Guidance on the assessment and monitoring of natural attenuation of contaminants in groundwater. Technical publication no. 95, pp. 131.

Eschenroeder, A.Q., Faeder, E.J., 1988. A Monte Carlo analysis of health risks from PCB-contaminated mineral oil transformer fires. Risk Anal. 8, 291–297.

Gelhar, L.W., Welty, C., Rehfeldt, K.R., 1992. A critical review of data on field-scale dispersion in aquifers. Water Resour. Res. 28, 1955–1974.

Goodrich, M.T., McCord, J.T., 1995. Quantification of uncertainty in exposure assessments at hazardous waste sites. Ground Water 33, 727–732.

Hass, C.N., Anotai, J., Engelbrecht, R.S., 1996. Monte Carlo assessment of microbial risk associated with landfilling of fecal material. Water Environ. Res. 68, 1123–1131.

Heron, G., Christensen, T.H., 1995. Impact of sediment-bound iron on redox buffering in a landfill leachate polluted aquifer (Vejen, Denmark). Environ. Sci. Technol. 29, 187–192.

Hess, A., Höhener, P., Hunkeler, D., Zeyer, J., 1996. Bioremediation of a diesel fuel contaminated aquifer: simulation studies in laboratory aquifer columns. J. Contam. Hydrol. 23, 329–345.

Hunkeler, D., Jorger, D., Haberli, K., Höhener, P., Zeyer, J., 1998. Petroleum hydrocarbon mineralization in anaerobic laboratory aquifer columns. J. Contam Hydrol. 32, 41–61.

Hunkeler, D., Höhener, P., Bernasconi, S., Zeyer, J., 1999. Engineered in situ bioremediation of a petroluem hydrocarbon-contaminated aquifer: assessment of mineralization based on alkalinity, inorganic carbon and stable carbon isotope balances. J. Contam. Hydrol. 37, 201–223.

James, A.L., Oldenburg, C.M., 1997. Linear and Monte Carlo uncertainty analysis for subsurface contaminant transport simulations. Water Resour. Res. 33, 2495–2508.

Jefferies, M., Hall, D., Hinchliff, J., Aitken, M., 1993. Risk assessment: where are we, and where are we going? In: Bentley, S.P. (Ed.), Engineering Geology of Waste Disposal. Geol. Soc. Eng. Geol. Spec. Publ., pp. 241–359.

Lyngkilde, J., Christensen, T.H., 1992. Fate of organic contaminants in the redox zones of a landfill leachate pollution plume (Vejen, Denmark). J. Contam. Hydrol. 10, 291–307.

Mayer, K.U., Benner, S.G., Frind, E.O., Thornton, S.F., Lerner, D.N., 2001. Reactive transport modelling of processes controlling the distribution and natural attenuation of phenolic compounds in a deep sandstone aquifer. J. Contam. Hydrol. 53, 341–368.

McNab, W.W., Dooher, B.P., 1998. Uncertainty analyses of fuel hydrocarbon biodegradation signatures in ground water by probabilistic modeling. Ground Water 36, 691–698.

Nicholson, R.V., Cherry, J.A., Reardon, E.J., 1983. Migration of contaminants in groundwater at a landfill: a case study: 6. Hydrochemistry. J. Hydrol. 63, 131–176.

Ravi, V., Chen, J.S., Gierke, W., 1997. Evaluating the natural attenuation of transient-source compounds in groundwater. Proc. Batelle Conference San Diego, pp. 205–211.

Schreiber, M.E., Bahr, J.M., 1999. Spatial electron acceptor variability: implications for assessing bioremediation potential. Biorem. J. 3, 363–378.

Skaggs, T.H., Kabala, Z.J., 1998. Limitations in recovering the history of a groundwater contaminant plume. J. Contam. Hydrol. 33, 347–359.

Spence, M.J., Bottrell, S.H., Thornton, S.F., Lerner, D.N., 2001. Isotopic modelling of the significance of sulphate for phenol attenuation in a contaminated aquifer. J. Contam. Hydrol. 53, 285–304.

Stumm, W., Morgan, J.J., 1996. Aquatic Chemistry, 3rd edn. Wiley, New York.

Thornton, S.F., Quigley, S., Spence, M., Banwart, S.A., Bottrell, S., Lerner, D.N., 2001. Processes controlling the distribution and natural attenuation of phenolic compounds in a deep sandstone aquifer. J. Contam. Hydrol. 53, 233–267.

Tuccillo, M.E., Cozzarelli, I.M., Herman, J.S., 1999. Iron reduction in the sediments of a hydrocarbon-contaminated aquifer. Appl. Geochem. 14, 655–667.

Wiedemeier, T.H., Downey, D.C., Wilson, J.T., Kampbell, D.H., Miller, R.N., Hansen, J.E., 1995. Technical Protocol for Implementing the Intrinsic Remediation (Natural Attenuation) with Long Term Monitoring Option for Dissolved-Phase Fuel Contamination in Groundwater. Air Force Center for Excellence, Brooks Air force Base, USA.

Williams, G.M., Pickup, R.W., Thornton, S.F., Lerner, D.N., Mallinson, H.E.H., Moore, Y., White, C., 2001. Biogeochemical characterisation of a coal tar distillate plume. J. Contam. Hydrol. 53, 175–198.